The mechanism of the electronic transition in ferroborates under high pressure

2005 J. Phys.: Condens. Matter 17 S743

(http://iopscience.iop.org/0953-8984/17/11/003)

J. Phys.: Condens. Matter **17** (2005) S743–S751 doi:10.1088/0953-8984/17/11/003

The mechanism of the electronic transition in ferroborates under high pressure

S G Ovchinnikov

L V Kirensky Institute of Physics, Siberian Branch of the Russian Academy of Science, Krasnoyarsk, 660036, Russia

E-mail: sgo@iph.krasn.ru

Received 5 January 2005
Published 4 March 2005
Online at stacks.iop.org/JPhysCM/17/S743

Abstract
A novel mechanism for the insulator–semiconductor transition and magnetic collapse in $FeBO_3$ is proposed in the framework of the multielectron model with account taken of strong electron correlations. The electronic transition results from the crossover of the high spin and low spin Fe^{3+} states induced by the crystal field increasing with pressure. In the high pressure phase a semiconductor–metal transition is expected.

1. Introduction

In many magnetic oxides both the localized magnetic moment (LMM) in the d^n configuration and the insulating electric properties arise due to strong electron correlation (SEC). Well-known examples showing this behaviour include NiO, MnO and, found more recently, La_2CuO_4 and $LaMnO_3$. The ferroborates $FeBO_3$ and $GdFe_3(BO_3)_4$ also belong to the group of systems with SEC. The simplest model for treating SEC is the Hubbard model, where LMM and insulating properties arise place in the SEC limit $U \gg W$ (U is the Hubbard intra-atomic Coulomb parameter, W is the half-bandwidth). With increasing pressure, U is assumed constant while W should increase. Thus a Mott–Hubbard antiferromagnetic insulator with $U \gg W$ under high pressure will transform into a non-magnetic metal with $U \leqslant W$. This idea has been used to study the magnetic collapse in FeO, MnO and CoO by *ab initio* methods [1]. We will call this situation bandwidth control, meaning that it is the $W(P)$ increase that results in the electronic and magnetic transition. We claim in this work that in ferroborates there is another mechanism governing the electronic transition, crystal field control. The cubic component of the crystal field $\Delta = \varepsilon(e_g) - \varepsilon(t_{2g}) \equiv 10Dq$ also increases with pressure due to the decreasing Fe–O distance. At some critical pressure P_C there is a crossover of the high spin (HS) $^6A_1$ and low spin (LS) $^2T_2$ terms of the Fe^{3+} ion. The change of the ground state of the d^5 and electron addition (removal) d^6 (d^4) configurations reduces the effective Hubbard U_{eff} and the energy gap in the single-electron density of states (DOS) [2].

Nevertheless, for a crystal both the bandwidth and the crystal field depend on the pressure, as do other parameters of the electronic structure. In this paper we analyse the electronic structure of $FeBO_3$ under high pressure, and estimate the $W(P)$ and $\Delta(P)$ dependences from the fitting to the experimental data. Experimental studies of $FeBO_3$ reveal a structural transition [3], collapse of the magnetic moment [4], a sharp decrease of the insulator gap and the optical gap [5] at $P_C = 47$ GPa.

The paper is organized as follows. The electronic structure of $FeBO_3$ in the multielectron model with account taken of SEC in the generalized tight binding (GTB) method [6] is given in section 2. Bandwidth control versus crystal field control and other changes in the electronic structure are discussed in section 3. Section 4 considers the magnetic collapse and the insulator–semiconductor transition at $P = P_C$. The electronic structure above P_C and a possible semiconductor–metal transition at $P = P_M > P_C$ are discussed in section 5. Finally, in section 6 we make concluding remarks.

2. The electronic structure of $FeBO_3$ in the multielectron model in the framework of the GTB method

The electronic structure of $FeBO_3$ at zero external pressure and the optical properties in the framework of this model have been discussed in [7]. Here we outline the essential part of the model, to be ready to discuss the effect of pressure.

The *ab initio* single-electron energy band calculations performed for $FeBO_3$ using the density functional method in the local spin density approximation [8] and the generalized gradient approximation [9] together with the calculation of molecular orbitals of a FeB_6O_6 cluster [10] revealed the following electron structure of $FeBO_3$. The empty conduction band ε_c consists predominantly of the s and p states of boron. The top of the valence band ε_v is formed mostly by the s and p states of oxygen. The energy gap E_{g0} between the valence and conduction bands in the antiferromagnetic phase amounts to 2.5 eV, which is quite close to the fundamental absorption edge ($E_{g0} = 2.9$ eV). A band of d electrons occurs at the top of the valence band, and the crystal field parameter is $\Delta \approx 1$ eV. The degree of hybridization of the d electrons of iron with the s and p electrons of oxygen is very small [8, 10], much smaller compared to the case for 3d metal oxides. This is related to a very strong hybridization inside the BO_3 group, where the $(BO_3)^{3-}$ ion does in fact exist and the electron orbitals of oxygen strongly overlap with the sp boron orbitals (which accounts for the small p–d hybridization). This circumstance significantly simplifies the multielectron model: the d^n ($n = 4, 5, 6$) terms of iron in the crystal field can be calculated, rather than the terms of a metal–oxygen complex (as for copper oxides [11]).

The Fe^{3+} ion has a d^5 configuration that can occur in various spin and orbital terms. The considerations below will also imply knowledge of the terms of d^4 (Fe^{4+}) and d^6 (Fe^{2+}) configurations for description of the hole and electron creation in the many-electron system. The energies of the terms in each of these d^n configurations are expressed via the Racah parameters A, B, C and the crystal field Δ [12].

There are small differences in these parameters among d^4, d^5, d^6 configurations (typically $\sim$10%) and we neglect this difference assuming A, B, C and Δ to be the same. These parameters at ambient pressure have been found in [7]: $A = 3.42$ eV, $B = 0.084$ eV, $C = 0.39$ eV, $\Delta = 1.57$ eV. Let $\{|n, \gamma\rangle\}$ be a full set of eigenstates of the d^n ions ($n = 4, 5, 6$ for $FeBO_3$) with γ including spin and orbital indices. In the GTB method we start with the exact diagonalization of the intracell part of the Hamiltonian. Due to the weakness of the p–d hybridization we neglect it and find $|n, \gamma\rangle$ eigenstates to be pure d^n terms with energies $E_{n\gamma}$

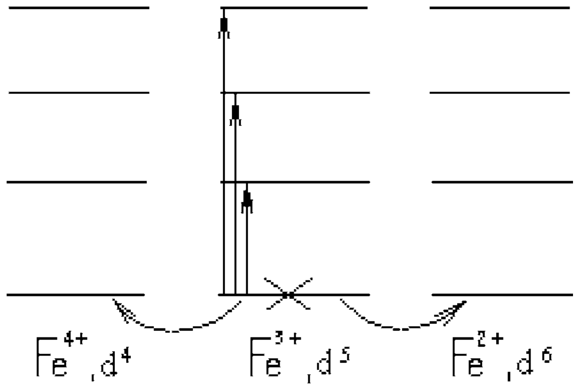

Figure 1. The scheme of neutral and charged d–d excitations in the d^4, d^5 and d^6 configurations.

determined from Tanabe–Sugano diagrams. We construct also the Hubbard X-operators

$$X^{n_1\gamma_1,n_2\gamma_2} = |n_1\gamma_1\rangle\langle n_2\gamma_2|. \tag{1}$$

For the Fe^{3+} ion the HS term ${}^6A_1$ has the minimal energy, and the minimal energy terms of the d^4 and d^6 configurations also have high spin:

$$\begin{aligned} E_0(d^4) &\equiv E({}^5E, d^4) = 4\varepsilon_d + 6A - 21B - 0.6\Delta, \\ E_0(d^5) &\equiv E({}^6A_1, d^5) = 5\varepsilon_d + 10A - 35B, \\ E_0(d^6) &\equiv E({}^5T_2, d^6) = 6\varepsilon_d + 15A - 21B - 0.4\Delta. \end{aligned} \tag{2}$$

Here ε_d is the atomic single-d-electron energy, split by the cubic crystal field to $\varepsilon(t_{2g}) = \varepsilon_d - 0.4\Delta$ and $\varepsilon(e_g) = \varepsilon_d + 0.6\Delta$.

In figure 1 we show different neutral d–d excitations (vertical arrows) inside Fe^{3+} ions and also charged excitations (horizontal arrows). The optical absorption peaks are associated with d–d excitations ${}^6A_1 \to {}^4T_1$, ${}^6A_1 \to {}^4T_2$, ${}^6A_1 \to {}^4A_1$. The addition of one extra d electron requires an energy

$$\Omega_C = E_0(d^6) - E_0(d^5). \tag{3}$$

Similarly, for removing a d electron the corresponding energy is

$$\Omega_v = E_0(d^5) - E_0(d^4). \tag{4}$$

A local quasiparticle energy of the form

$$\Omega^{\gamma_1\gamma_2} = E_0(n_1, \gamma_1) - E_0(n_1 - 1, \gamma_2)$$

is a natural result of the Hubbard X-operator algebra and may be considered as a generalization of Landau Fermi liquid ideas to non-Fermi liquid systems with SEC. The energies Ω_C and Ω_v are similar to the upper and low Hubbard bands in the Hubbard model. The effective Hubbard parameter U_{eff} can be determined as follows:

$$U_{eff} = E_0(d^4) + E_0(d^6) - 2E_0(d^5) = A + 28B - \Delta. \tag{5}$$

For the parameters given above, we find $U_{eff} = 4.2$ eV.

The second step in the GTB method is to write the Fermi operator of d electron creation with orbital λ and spin σ in the X-operator representation:

$$d^+_{f\lambda\sigma} = \sum_{n,\gamma_1,\gamma_2} \nu_{\lambda\sigma}(n, \gamma_1, \gamma_2) X_f^{n\gamma_1;n-1,\gamma_2},$$

and to treat the interatomic hopping

$$H_t = \sum_{fg} \sum_{\gamma_1\gamma_2\sigma} t_{fg}^{\gamma_1\gamma_2} d_{f\gamma_1\sigma}^{+} d_{g\gamma_2\sigma} \tag{6}$$

by methods reliable in the SEC limit $U_{\text{eff}} \gg W$ [6].

In the nearest neighbour approximation $W = zt$, where z is the number of nearest neighbours ($z = 6$ for $FeBO_3$) and t is the parameter for hopping between two Fe ions. The hopping occurs via intermediate oxygen, $t \sim (t_{\text{pd}})^2/|\varepsilon_{\text{p}} - \varepsilon_{\text{d}}|$, where t_{pd} is the Fe–O hopping, ε_{p} and ε_{d} are the atomic energies of oxygen p and Fe d electrons. The weakness of the p–d hybridization discussed above means a small value of t_{pd} and a narrow d band. The *ab initio* LDA calculations [8, 13] give for the t_{2g} band $W_0 \approx 1$ eV. The LDA is known to overestimate the bandwidth in SEC systems. That is why we estimate the hopping t from the experimental data for the Néel temperature.

The effective exchange Fe–Fe can be estimated as

$$J = 2t^2/U_{\text{eff}} \tag{7}$$

and the Néel temperature in the mean field approximation is

$$T_{\text{N}} = JzS(S+1)/3. \tag{8}$$

With $T_{\text{N}} = 350$ K for $FeBO_3$ we find $J = 20$ K. From fitting the Mössbauer effect data to the spin wave theory, Eibschütz and Lines [14] obtained $J = 27.3$ K in very good agreement with the Rushbrooke and Wood [15] high temperature series expansion. The simplest mean field estimation for J is quite close to the ones obtained by more elaborate methods. We estimate t from equation (7) to be $t = \sqrt{JU_{\text{eff}}/2} = 0.06$ eV, and for the half-bandwidth $W_0 = 0.36$ eV. This is a free electron bandwidth. In the antiferromagnetic state the hopping between nearest neighbours is strongly suppressed by the spin polaron effect and requires spin fluctuations; the effective hopping $t_{\text{eff}} = t\sqrt{n_0(1-n_0)}$, where $n_0 = S - \langle S^z \rangle$ [16]. For $S = 5/2$ the zero-point magnon fluctuations result in a 3D antiferromagnet with $n_0 = 0.078$ [17]. Thus $t_{\text{eff}} = 0.27t = 0.016$ eV and $W_{\text{eff}} \approx 0.1$ eV. These estimations show that due to the many-body effects the d electron bandwidth is small, of the order of 0.1 eV. A small bandwidth $\sim$0.1 eV is in agreement with optical absorption data where the typical linewidth is small. To finish the discussion of the bandwidth in $FeBO_3$, we emphasize that it is very small in comparison to those of mono-oxides such as NiO, FeO, due to the small p–d hybridization. This is specific to boroxides; for mono-oxides the p–d hybridization is quite large and $W \sim 1$ eV.

We will take into account the bandwidth effect by broadening the δ-function peaks in the DOS. The DOS for $FeBO_3$ at ambient pressure is shown in figure 2(a) [7]. The electronic structure of $FeBO_3$ is that of a change transfer insulator with the minimal excitation energy

$$E_{\text{g}}^{\text{CT}} = \Omega_{\text{C}} - \varepsilon_{\text{v}} - W_{\text{eff}} \tag{9}$$

corresponding to the charge transfer excitation $p^6d^5 \rightarrow p^5d^6$.

3. Bandwidth versus crystal field control of the electronic structure under high pressure

With decreasing interatomic distances we assume $t(P)$ and $\Delta(P)$ to be linearly increasing:

$$t(P) = t_0 + \alpha_t P, \qquad \alpha_t = \partial t/\partial P, \tag{10}$$

$$\Delta(P) = \Delta_0 + \alpha_\Delta P, \qquad \alpha_\Delta = \partial\Delta/\partial P. \tag{11}$$

All intra-atomic parameters that enter the theory (Raccah parameters A, B, C) we assume to be pressure independent. The band gap $E_{\text{g0}} = \varepsilon_{\text{c}} - \varepsilon_{\text{v}}$ we also assume not to depend on

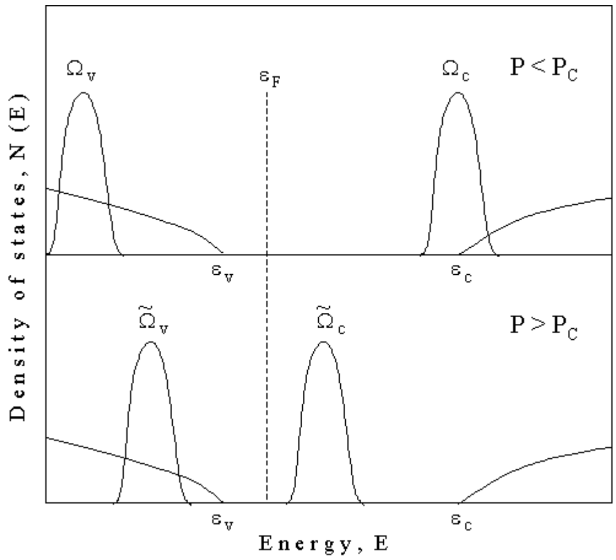

Figure 2. Densities of states of $FeBO_3$ at low (a) and high (b) pressure.

pressure because the absorption edge remains constant when pressure increases [18]. The effective Hubbard parameter, as can be seen from equations (5) and (10), will decrease with pressure:

$$U_{\rm eff}(P) = U_0 - \alpha_\Delta P. \tag{12}$$

With pressure, the $S = 1/2$ LS term $^2T_2$ of the Fe^{3+} ion decreases in energy very quickly (figure 3), and the $^2T_2$–$^6A_1$ term crossover takes place at $P = P_C$ where $\Delta(P_C) \equiv \Delta_C$. From figure 3, $\Delta_C = 28.5B = 2.4$ eV, and using the experimental value of $P_C = 46$ GPa we obtain $\alpha_\Delta = (\Delta_C - \Delta_0)/P_C = 0.018$ eV GPa^{-1}.

The parameter α_t can be found from the pressure dependence of the Néel temperature. Experimentally, it increases linearly up to $T_N^{(-)}(P_C) = 600$ K (here 'minus' means the value from the left at P_C, because of the sharp drop of T_N at P_C). The increase of t and decrease of $U_{\rm eff}$ result in increasing of T_N:

$$T_N(P)/T_N(0) = 1 + (2\alpha_t/t_0 + \alpha_\Delta/U_0)P. \tag{13}$$

From equation (13) we find $\alpha_t = 0.000\,33$ eV GPa^{-1}. The effective bandwidth just below the transition is

$$W_{\rm eff}(P_C) = Zt_{\rm eff}(P_C) = Z\sqrt{n_0(1-n_0)}(t_0 + \alpha_t P_C) = 0.12 \text{ eV}. \tag{14}$$

So with 20% growth the bandwidth is still very small and cannot be the driving force for the transition. In contrast, the crystal field parameter Δ has a very large increase. All the optical absorption lines $\omega_A = E(^4T_1) - E(^6A_1)$, $\omega_B = E(^4T_2) - E(^6A_1)$ and $\omega_C = E(^4A_1) - E(^6A_1)$ decrease in energy with pressure; the derivatives $d\omega_i/dP$ have been calculated in this model and found to be in reasonably good agreement with the experimental data [18]. Thus we may conclude that there is indeed crystal field control of the electronic structure evolution with pressure in $FeBO_3$, both due to the smooth decreasing of $U_{\rm eff}$ with Δ in equation (5) and the abrupt decrease of $U_{\rm eff}$ at P_C due to the HS–LS crossover.

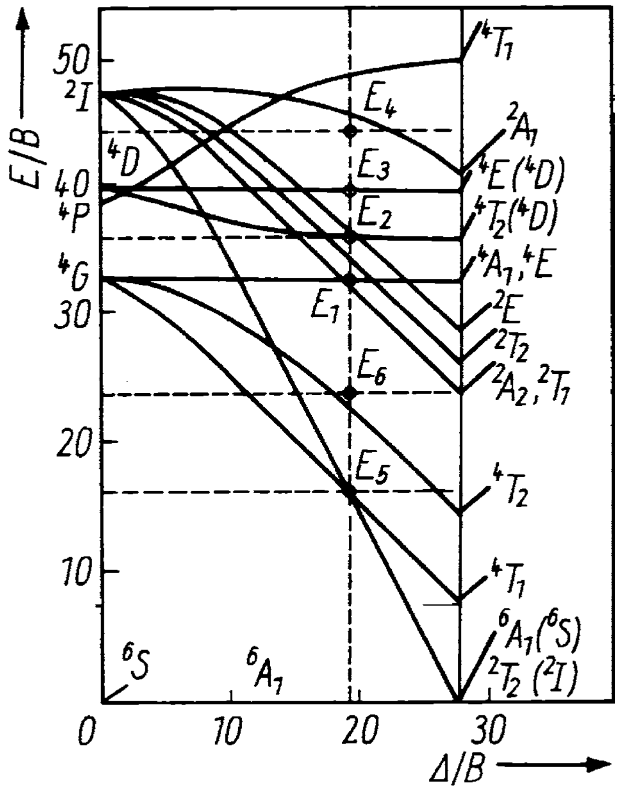

Figure 3. The Tanabe–Sugano diagram for the Fe^{3+} ion. A dashed line corresponds to the $FeBO_3$ parameters (after [19]).

4. Magnetic collapse and the insulator–semiconductor transition

Near the crossover we can write down the sublattice magnetization

$$\langle S^z \rangle = 5/2 n_{5/2}(P, T) + 1/2 n_{1/2}(P, T), \quad (15)$$

where $n_S(P, T)$ is a weight factor for the term with spin S. It is given by ($\Delta E = E_{1/2} - E_{5/2}$)

$$n_{5/2} = [1 + \exp(-\Delta E/kT)]^{-1},$$

$$n_{1/2} = \exp(-\Delta E/kT)[1 + \exp(-\Delta E/kT)].$$

These factors at $T = 0$ change discontinuously at P_C (figure 4). Above P_C the magnetic moment of Fe^{3+} is not zero and its spin value is 1/2, so the term ‘collapse’ means here not the disappearance of magnetism but a dramatic decrease of the magnetization and the Néel temperature. From the Tanabe–Sugano diagrams for Fe^{4+} and Fe^{2+} ions we can note that at $\Delta < \Delta_C$ similar crossovers have occurred: for Fe^{4+} HS ^5E and LS $^3T_1$, and for Fe^{2+} HS $^5T_2$ and LS $^1A_1$. Thus at $P > P_C$ the lowest energy terms are

$$\begin{aligned} &Fe^{4+}: {}^3T_1, S = 1, \\ &Fe^{3+}: {}^2T_2, S = 1/2, \\ &Fe^{2+}: {}^1A_1, S = 0; \end{aligned} \quad (16)$$

with these terms the energies of the upper and low Hubbard bands change:

$$\tilde{\Omega}_C = E(^1A_1, d^6) - E(^2T_2, d^5), \quad (17)$$

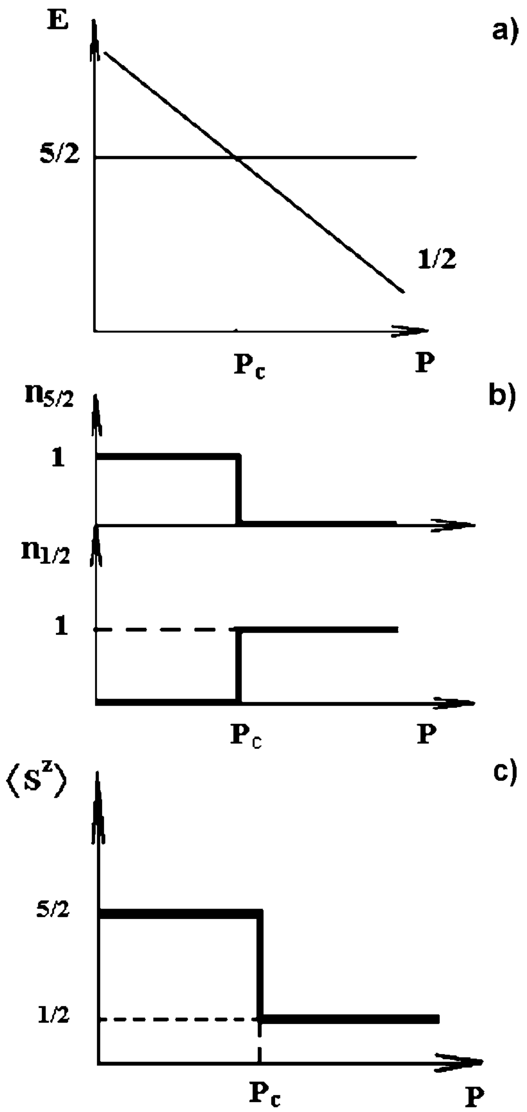

Figure 4. The mechanism of magnetic collapse due to high spin–low spin term crossover.

$$\tilde{\Omega}_v = E(^2T_2, d^5) - E(^3T_1, d^4), \tag{18}$$

and the effective U given by equation (5) also changes:

$$\tilde{U}_{eff} = \tilde{\Omega}_C - \tilde{\Omega}_v = A + 9B - 7C. \tag{19}$$

We obtain the jump of U_{eff} at the transition: at $P > P_C$, $\tilde{U}_{eff} = 1.45$ eV. Thus the electron correlation drastically decreases at the transition; the DOS at $P > P_C$ is given in figure 1(b). The energy gap (9) sharply decreased from 3 eV at $P < P_C$ to 0.8 eV at $P > P_C$. That is why the magnetic collapse is accompanied by an insulator–semiconductor transition.

Note that we do not discuss here the isostructural phase transition of first order at $P = 53$ GPa with a 9% drop of the unit cell volume [3]. Up to now it has not been clear whether this is the same as the electronic transition at $P_C = 47$ GPa or not. The mechanism of structural phase transition has been studied by Parlinski [9] in the framework of the GGA to the density functional theory.

5. Electronic properties in the high pressure phase

The effective U above P_C (equation (19)) does not depend on Δ and pressure. The upper Hubbard band $\tilde{\Omega}_C$ decreases in energy with P:

$$d\tilde{\Omega}_C/dP = -0.4\alpha_\Delta = -0.0072 \text{ eV GPa}^{-1}. \tag{20}$$

The charge transfer gap will also decrease:

$$E_g(P) = E_g(P_C) + (P - P_C)\, dE/dP$$
$$= \tilde{\Omega}_C(P_C) - W_{eff}(P_C) - \varepsilon_v - (P - P_C)\big(0.4\alpha_\Delta + 6\alpha_t\sqrt{n_0(1-n_0)}\big). \tag{21}$$

The extrapolation of the gap to zero gives the second electronic transition, the semiconductor–metal transition at $P = P_M$. From equation (21) we can estimate $P_M = 143$ GPa. Experimental study of the resistivity of $FeBO_3$ up to 140 GPa has not revealed a metal phase; the extrapolated value $P_M^{exp} \approx 200$ GPa [5]. The accuracy of the extrapolation (21) to the high pressure region is not high. First, we do not know when the non-linear contribution to the $\Delta(P)$ dependence will become important. Second, we assume for simplicity that the top of the valence band ε_v does not depend on energy, and in the low pressure phase this assumption is quite reasonable. Nevertheless, even a small shift of ε_v with $\delta\varepsilon_v \sim 0.1$ eV may shift P_M to 200 GPa. What we are sure of is the decrease in the charge transfer gap with pressure.

Above P_M the narrow d band $\tilde{\Omega}_C$ will cross the top of the valence band, ε_v. Some oxygen holes will appear at $\varepsilon < \varepsilon_v$. The iron will be in the mixed valence state given by a mixture of $d^5(S = 1/2)$ and $d^6(S = 0)$ configurations. The proper model for this physics seems to be the periodic Anderson model.

The magnetic properties above P_C are determined by the LS Fe^{3+} term with $S = 1/2$. Assuming the exchange parameter J to be continuous at P_C, we can estimate

$$T_N^{(+)} = 3T_N^{(-)}/35 = 51 \text{ K}. \tag{22}$$

At $P > P_C$, $T_N(P)$ will linearly increase with a slope $2\alpha_t/t_0$ smaller than that in the low pressure phase (because $\tilde{U}_{eff}$ does not depend on P).

Close to metallization at $P = P_M$, the Heisenberg model approach becomes inappropriate and magnetic properties should be considered in the framework of the periodic Anderson model.

6. Conclusion

The multielectron approach to the electronic structure that we used in this work is rather general and can be applied to various d and f metal oxides. The initial formulation of the GTB method [11] has been used to study cuprates. The ferroborate $FeBO_3$ is particular only in having a very small Fe–Fe hopping due to the small Fe d–O p hybridization. Another similar crystal is $GdFe_3(BO_3)_4$, where FeO_6 distorted octahedra have an Fe–O distance almost the same as that in $FeBO_3$.

The mechanism of magnetic transition with high spin–low spin crossover is well known and has been discussed many times, for example by Hearne *et al* [20] for $LaFeO_3$. The novelty in our approach is the simultaneous change in the electronic structure that requires one to go beyond the Fe^{3+} configuration and include d electron addition and removal (Fe^{2+} and Fe^{4+}) configurations as well.

Acknowledgments

I am grateful to I S Lyubutin, A G Gavriliuk, V A Sarkisyan, D I Khomskii, M M Abd-Elmeguid for stimulating discussions. This work was supported by RFBR grant 03-02-16286 and the Programme 'Strongly correlated electrons' of the Physical Branch of the Russian Academy of Sciences.

References

[1] Cohen R E, Mazin I I and Isaak D G 1997 *Science* **275** 654
[2] Ovchinnikov S G 2003 *JETP Lett.* **77** 676
[3] Gavriliuk A G *et al* 2002 *JETP Lett.* **75** 23
[4] Sarkisyan V A *et al* 2002 *JETP Lett.* **76** 664
[5] Trojan I A *et al* 2003 *JETP Lett.* **78** 13
[6] Ovchinnikov S G and Val'kov V V 2004 *Hubbard Operators in the Theory of Strongly Correlated Electrons* (London: Imperial College Press)
[7] Ovchinnikov S G and Zabluda V N 2004 *JETP* **98** 135
[8] Postnikov A V *et al* 1994 *Phys. Rev.* B **50** 14849
[9] Parlinski K 2002 *Eur. J. Phys.* B **27** 283
[10] Ivanova N B *et al* 2002 *JETP* **94** 299
[11] Gavrihkov V A, Ovchinnikov S G, Borisov A A and Goryachev E G 2000 *JETP* **91** 369
[12] Tanabe Y and Sugano S 1954 *J. Phys. Soc. Japan* **9** 766
[13] Ovchinnikov S G, Anisimov V I, Nekrasov I A and Pchelkina Z V 2004 *EASTMAG-2004: Abstracts of Euro-Asian Symposium Trends in Magnetism (Krasnoyarsk, Russia, Aug. 2004)*
[14] Eibschütz M and Lines M E 1973 *Phys. Rev.* B **7** 4907
[15] Rushbrooke G S and Wood P J 1963 *Mol. Phys.* **6** 409
[16] Ovchinnikov S G 1995 *JETP* **80** 451
[17] Anderson P W 1952 *Phys. Rev.* **86** 694
[18] Gavriliuk A G *et al* 2004 *JETP* **99** 566
[19] Malakhovskii A V and Edelman I S 1976 *Phys. Status Solidi* b **74** K145
[20] Hearne G R, Pasternak M P, Taylor R D and Lacorre P 1995 *Phys. Rev.* B **51** 11495